Hemin-Stimulated Docking of Cytochrome *c* to a Hemin−DNA Aptamer Complex†

Daniel J. F. Chinnapen and Dipankar Sen*

Department of Molecular Biology and Biochemistry, Simon Fraser University, Burnaby, British Columbia, V5A 1S6, Canada

Received September 19, 2001

ABSTRACT: DNA aptamers were selected for their ability to bind simultaneously to the protein cytochrome *c* and to the metalloporphyrin hemin. Such aptamers each contained a conserved guanine-rich core, analogous to sequences shown previously to form a hemin-binding site when folded. The detailed study of CH6A, a deletion mutant of one clone, indicated that in the presence of hemin the guanine-rich core of the aptamer folded to form a guanine quadruplex. Both hemin and potassium ions were required for this folding. The binding of fully oxidized cytochrome *c* to this DNA−hemin complex resulted in an absorbance difference spectrum in the Soret region, which could be used as an indicator of binding behavior. It was found that cytochrome *c* bound more tightly to the folded CH6A DNA−hemin complex than to the folded CH6A DNA alone. A single hemin molecule and a single cytochrome *c* bound to each molecule of folded CH6A. Footprinting experiments showed the binding site of the cytochrome *c* to be a partial duplex element of the aptamer, immediately flanking its guanine-rich hemin-binding site. The order of addition of hemin and cytochrome *c* appeared not to affect either the formation rate or the structure of the final ternary complex. The ternary complex represents the docking of a nucleic acid−heme complex to cytochrome *c* (a protein−heme complex). Future experiments will focus on investigating the optimal electron-transfer path between the two iron centers through intervening protein and DNA.

A number of important redox processes in biology involve the transfer of electrons between two docked iron(III) protoporphyrin IX (hemin)[1]-containing proteins. Cytochrome *c* is one such protein that has been well characterized and is known to bind to many different protein redox partners, such as cytochrome b_5, cytochrome *c* oxidase, and cytochrome *c* peroxidase (*1*). Cytochrome *c* has also been the subject of much study recently, because of its implicated role in apoptosis (*2*−*4*). The interaction between cytochrome *c* and another heme-containing protein, cytochrome b_5 (reviewed in *5*), in particular, has been intensively researched and has become a model for the study of interactions between two redox proteins. Recently, novel charge-transfer interactions have also been reported between cytochrome *c* and ruthenium-intercalated double-stranded DNA (*6*).

Single-strand DNA and RNA "aptamers", obtained by selection from random-sequence DNA/RNA libraries, have previously been shown to bind to a variety of target ligands as well as catalyze a variety of reactions normally catalyzed by proteins in cells (reviewed in *7*, *8*). Some examples of such reactions catalyzed include phosphodiester bond cleavage (*9*), DNA 5′-capping (*10*), and nucleotide synthesis (*11*). DNA enzymes have also been described, for which porphyrins act as either cofactor or substrate. Li and Sen (*12*−*14*) reported a porphyrin-metallating DNA enzyme, PS2.M, 18 nucleotides long, capable of catalytically inserting zinc and copper(II) ions into mesoporphyrin IX or protoporphyrin IX. Interestingly, this same DNA oligonucleotide, when complexed with hemin, catalyzed peroxidation reactions utilizing hydrogen peroxide (*15*−*18*). Given the ability of DNA to accomplish these two types of porphyrin-utilizing reactions normally attributed to proteins, it would be interesting to see if DNA could also participate in electron-transfer reactions comparable to those seen with cytochrome proteins.

We wished to investigate whether a hemin-binding DNA molecule could also bind to cytochrome *c*, specifically and with relatively high affinity. Within cells, the basic protein cytochrome *c* is known to dock with the acidic cytochrome b_5 to initiate electron transfer (*5*, *19*). Ostensibly, the binding of DNA to cytochrome *c* could be mediated purely by Coulombic interactions between the positively charged lysine side chains of cytochrome *c* and the negative phosphate backbone of DNA. However, such an interaction might be nonspecific and lead to unpredictable binding stoichiometries. For this reason, it would be important to select for DNA binders of cytochrome *c* at relatively high salts, to encourage a more specific binding. The goal overall, then, would be to select DNA aptamers capable of binding simultaneously to the small molecule hemin and to the protein cytochrome *c*. From our earlier investigations on DNA enzymes utilizing porphyrins as either substrate or cofactor (see above), we had obtained a pool of DNA molecules (the "PS" pool) with a propensity to bind to porphyrins. This unsorted collection of DNA molecules was therefore subjected to a secondary selection process for the ability to bind cytochrome *c*.

† This work was supported by the Natural Sciences and Engineering Research Council of Canada (NSERC).

* To whom correspondence should be addressed at the Department of Molecular Biology and Biochemistry, Simon Fraser University, 8888 University Dr., Burnaby, BC V5A 1S6, Canada. Tel: 604-291-4386. Fax: 604-291-5583. E-mail: sen@sfu.ca.

[1] Abbreviations: hemin, iron(III) protoporphyrin IX; ATP, adenosine triphosphate; DEPC, diethyl pyrocarbonate; DMS, dimethyl sulfate; DMSO, dimethyl sulfoxide; FMN, flavin mononucleotide; H_2O_2, hydrogen peroxide; PCR, polymerase chain reaction; PS2M, a small guanine-rich oligonucleotide (5′-GT GGT AGG GCG GGT TGG-3′); SELEX, Systematic Evolution of Ligands by Exponential Enrichment; Tris, tris(hydroxymethyl)aminomethane.

10.1021/bi015785f CCC: $22.00
Published on Web 03/27/2002

MATERIALS AND METHODS

Materials. Hemin was purchased from Porphyrin Products (Logan, UT) and was used without further purification. Horse heart ferricytochrome *c* was obtained from Sigma and purified by the method of Brautigan et al. (*20*) on CM-cellulose. The purified cytochrome *c* was fully oxidized with potassium ferricyanide and the solution passed through a G-25 Sephadex column to remove ferricyanide. Hemin-agarose beads, agarose beads, and epoxy-activated Sepharose 6B were purchased from Sigma. Cloning was performed with a TA cloning kit and One-shot competent cells from Invitrogen. [γ-^{32}P]ATP and the Thermo-sequenase ^{33}P dideoxy sequencing kit were from USB/Amersham. DNA oligonucleotides were purchased from Nucleic Acids Protein Services (NAPS) at the University of British Columbia. The control oligonucleotide PS2M used in spectrophotometric titrations had the sequence 5′-GT GGT AGG GCG GGT TGG-3′. The control peptide ADP-1 was purchased from United Biochemical Research, Inc. (Seattle, WA), and had the sequence: NH_2-CFTTK ALGIS YGRKK RRQRR RPPQG SQTHQ VSLSKQ-COOH.

DNA Library and Oligomers. A pool of DNA molecules (the "PS" pool) from a previous in vitro selection (*12*) for the binding of *N*-methylmesoporphyrin (NMM) was used as the starting pool for this selection. These DNA molecules were of the sequence 5′-GGA TCT TTT TGA TCG GTC GGC ACC -N_{76}- CCT TGG GTC ATT AGG CGA-3′. The primers R1P1-biotin (5′-biotin-TCG CCT AAT GAC CCA AGG) and RLS (5′-GGA TCT TTT TGA TCG GTC GGC ACC-3′) were used to amplify these molecules between rounds of selection, and the amplified DNA was internally labeled with [α-^{32}P]dATP. Amplified double-stranded DNA was size-purified in 8% nondenaturing gels.

Single-stranded DNA was prepared by binding the amplified double-stranded sequences to an avidin-agarose column in avidin-binding buffer (50 mM Tris-HCl, pH 8, 200 mM NaCl, 0.1 mM EDTA). The column was washed with 20 volumes of binding buffer. Single-stranded DNA molecules (the nonbiotinylated strand of the column-immobilized duplexes) were eluted with 500 μL of 0.2 M NaOH, directly into 100 μL of 50 mM Tris-HCl containing 1 M HCl to neutralize the basicity of the sample. The single-stranded DNA obtained was then ethanol-precipitated.

Selection Columns. Hemin-agarose beads were washed and preequilibrated in selection buffer A (50 mM Tris, pH 8.0, 120 mM NaCl, 20 mM KCl, 1% DMSO, 0.03% Triton X-100). Cytochrome *c* was attached to activated epoxy Sepharose 6B beads containing a 12-atom spacer. Excess cytochrome *c* was linked to the beads in protein coupling buffer (5 mM sodium phosphate, pH 7.0, 10 mM sodium chloride) by shaking for 72 h in the dark at room temperature. Protein attachment to the beads was periodically monitored by measuring the decrease in solution protein absorbance at 408 nm. The beads were then washed with 20 column volumes of storage buffer (80 mM sodium phosphate, pH 7), and stored in this buffer. Chemically blocked beads for negative selection columns were prepared by reacting the beads with 4% β-mercaptoethanol and shaking overnight. The beads were then washed and stored in storage buffer at 4 °C.

Selection Protocols. The selection strategy involved four columns: two positive columns, containing hemin and cytochrome *c*, respectively, and two negative columns, containing the respective beads—in the case of the Sepharose, chemically blocked. A single round of selection typically involved the following: ^{32}P-end-labeled single-stranded DNA molecules were heated to 95 °C for 5 min in TE buffer (10 mM Tris-HCl, pH 8, 0.1 mM EDTA) and allowed to cool very slowly for 25 min. For the first round of selection, an equal volume of 2× selection buffer A (see above) was added, and the DNA was allowed to fold for 30 min at room temperature. The folded DNA was then passed through a negative column containing blocked-agarose beads. DNA molecules that did not bind to this column were directly passed into a hemin-agarose column, the flow-through from this second column being recirculated through the column 5 times. Following 30 min of incubation, the hemin-agarose column was washed with selection buffer B (50 mM Tris, pH 8.0, 240 mM NaCl, 20 mM KCl, 1% DMSO, 0.03% Triton X-100) until no more counts were detectable in the eluate. The DNA molecules bound to this column were then eluted with TE buffer (10 mM Tris-HCl, pH 8, 10 mM EDTA).

The recovered DNA was ethanol-precipitated and refolded in reaction buffer. Hemin was added to a concentration of 8 μM (in at least a 10-fold molar excess over the DNA). These folded DNA molecules in the presence of the excess hemin were then passed through a second negative column containing blocked Sepharose (without cytochrome *c* attached). The unbound DNA was passed directly through a positive column containing cytochrome *c*-linked beads. As above, the flow-through was recirculated 5 times, and the beads and DNA solution were incubated for 30 min each time. The column was then washed with reaction buffer until no more counts were detected, and the bound DNA was eluted with a high-salt buffer, 2 M NaOAc (pH 6.0), followed by a TE buffer elution, so as not to bias the selection toward electrostatic interaction. In rounds 5 and 6, elution was achieved by incubation of the DNA-bound cytochrome *c* beads with free cytochrome *c* (2.5 mM) in selection buffer B. The eluted DNA−cytochrome solution was then phenol−chloroform-extracted and ethanol-precipitated, and the purified DNA was amplified by PCR using the R1P1-biotin and RLS primers.

Cloning and Sequencing. After round 6 of selection, the pool of DNA molecules successfully binding to the cytochrome *c* column was amplified using the cloning primers RLC (5′-CTT GTC TGC AGG GAT CCT TTT GAT CCG GTC GGC) and R1P1C (5′-GAT ATC AAG CTT CTC GAG TCG CCT AAT GAC CAA GG). The amplified DNA was gel-purified in an 8% nondenaturing gel and ligated into the pCR2.1 plasmid using a TA cloning kit (Invitrogen). The plasmid was then transformed into INVαF′ (Invitrogen) competent *E. coli* cells. Thirty-eight recombinant clones were picked for analysis and sequenced using the Thermo-sequenase dideoxy kit (USB Amersham). Sequence alignment was performed with the aid of the FOLDALIGN algorithm (*21*, *22*) to identify secondary structure conservation.

Dissociation Constant Determinations. The binding affinity for hemin of the various DNA aptamers was determined spectroscopically (*14*, *15*), by monitoring hyperchromicity of the hemin Soret absorption. All electronic absorption spectra were recorded in a dual-beam Cary 300-Bio UV−Visible Spectrophotometer, at 22 °C. The change in absor-

bance at 404 nm for hemin was monitored at increasing concentrations of DNA (0−20 μM) titrated to a fixed concentration (1.5 μM) of hemin in selection buffer A. The data obtained were fit to a binding equation by Wang et al. (*23*):

$$[\mathrm{DNA}]_o = K_d(A - A_o)/(A_\infty - A) + [\mathrm{P}_o](A - A_o)/(A_\infty - A_o)$$

where $[\mathrm{DNA}]_o$ is the starting concentration of DNA and A_o and A_∞ are the absorbances of DNA−hemin at zero concentration of DNA and at saturating concentrations of DNA, respectively. $[\mathrm{P}_o]$ is the initial concentration of monomeric hemin.

Binding constants for cytochrome *c* were also determined by difference absorption spectroscopy (*24*−*26*) using matched Hellma cuvettes and a dual-beam UV−visible Spectrophotometer (Varian). Measurements in the absence of hemin were carried out with only selection buffer in cuvette A, and 1.0 μM DNA in the same buffer in cuvette B. Then 0−7.6 μM cytochrome *c* was added to the DNA in cuvette B and the added absorbance spectrum of both cuvette A and cuvette B recorded as "Spectrum 1". The comparison run consisted of cuvettes C and D, both filled with buffer, with cuvette C containing 1.0 μM DNA. Cytochrome *c* (0−7.6 μM) was now added to cuvette D and the added spectrum of cuvettes C and D recorded as "Spectrum 2". Spectrum 2 was subtracted from Spectrum 1 to give the difference spectrum. Due to the sensitivity of the electronic spectra of both hemin and cytochrome *c* to their respective oxidation states (*27*), titrations were performed under oxidizing conditions in the presence of 10 μM potassium ferricyanide. All cuvettes were weighed on an analytical balance to an accuracy of ±0.0005 g prior to the recording of absorbance values. Spectra measured in the presence of hemin were recorded as above, except that 10 μM hemin was added to both cuvette B (with DNA and cytochrome *c* already present) for the sample run and to cuvette D (containing cytochrome *c* alone) for the blank run. No significant difference spectrum was observed for a titration of a fixed concentration of hemin with cytochrome *c*, relative to buffer, with a maximum ΔA_{408} of 0.0005 (in other words, any putative interaction of hemin with cytochrome *c* did not yield a difference spectrum). Binding constants of cytochrome *c* with DNA or with DNA−hemin were determined using a modified equation by Erman and Vitello (*24*):

$$\Delta A = \Delta A_\infty/2D\{C + D + 1/K_A - [(C + D + 1/K_A)^2 - 4CD]^{1/2}\}$$

where *C* and *D* are the concentrations of cytochrome *c* and DNA, respectively, ΔA_∞ is the change in absorbance at saturating concentrations of cytochrome *c*, and K_A is the association constant. Concentrations were corrected for dilution effects resulting from additions to the cuvettes from the cytochrome *c* stock. Three sets of independent measurements were taken.

Chemical Probing with Dimethyl Sulfate and Diethyl Pyrocarbonate. For methylation reactions, a 1.2% dimethyl sulfate (DMS) solution in water was freshly prepared and 1 μL added to 11 μL of 5′-kinased DNA folded in methylation buffer (20 mM potassium cacodylate, pH 8, 120 mM NaCl, 0.5% DMSO, and 0.03% Triton). For diethyl pyrocarbonate (DEPC) reactions, 5 μL of 3% DEPC was added to 10 μL of a DNA solution in the same buffer. Both reactions were allowed to proceed for 30 min at room temperature, and terminated by ethanol precipitation at dry ice temperatures. The recovered DNA was dissolved in 10% piperidine and heated for 30 min at 90 °C, followed by lyophilization. The samples were then dissolved in denaturing gel loading buffer (containing 80% formamide, v/v, and 20 mM EDTA, pH 8.0) and analyzed in 10% denaturing polyacrylamide gels.

Fenton Reaction Footprinting. The cleavage of DNA by Fenton reaction-generated hydroxyl radicals was performed using a method modified from Weidner et al. (*28*). 5′-Kinased DNA molecules were folded in selection buffer A, containing 20 mM KCl and 120 mM NaCl in a total volume of 10 μL. The solutions were then made up to 50 μM $Fe(NH_4)_2(SO_4)_2$, 100 μM EDTA, 1 mM sodium ascorbate, and the reaction was initiated by the addition of 10 mM H_2O_2 (final). After 1 min of reaction at room temperature, the samples were quenched by the addition of 2 μL of 5 mM thiourea. Solutions containing protein were phenol−choroform-extracted. The DNA solutions were then lyophilized, resuspended in denaturing gel-loading buffer, and analyzed in a 10% denaturing gel. It was ensured that equal radioactive counts were loaded into every well.

Table 1: Summary of Binding to Selection Columns

	% binding	
round	hemin beads	cyt *c* beads
1	49	<1
2	74	5[a]
3	73	15
4	ND	37
5	ND	50[b,c]
6	65	53[c]

[a] Total monovalent salt was increased from 140 to 260 mM. [b] Additional step added. DNA folded in the absence of hemin was passed through the cyt *c* column. Less than 5% of the DNA bound to the column, and the unbound DNA was then amplified for round 6. [c] 2.5 mM cytochrome *c* in selection buffer B was used to competitively elute the DNA off the column.

RESULTS

Selection. As described above, prior selections carried out in our laboratory to select for DNA enzymes that utilized porphyrins as either substrate or cofactor (see above) had generated, after 13 rounds of selection, a pool of DNA molecules (the "PS" pool) with a propensity to bind to porphyrins. It was impossible to estimate the number of individual sequences present in this PS pool; however, the sequencing of 25 cloned members from this pool had yielded 25 different sequences (*12*). Individual aptamers from this pool were also shown to be able to bind a variety of porphyrins and metalloporphyrins other than the *N*-methyl mesoporphyrin (NMM) used for that selection. This present selection was therefore one for a secondary binding activity, to cytochrome *c*, of DNA aptamers already predisposed to binding porphyrins.

Table 1 summarizes the binding of the PS pool DNA to the hemin and cytochrome *c* selection columns, as functions of rounds of selection. While the first round of selection was carried out in selection buffer A (50 mM Tris, pH 8.0, 120 mM NaCl, 20 mM KCl, 1% DMSO, 0.03% Triton X-100), in subsequent rounds the sodium chloride concentration was raised from 120 to 240 mM (selection buffer B), in an attempt

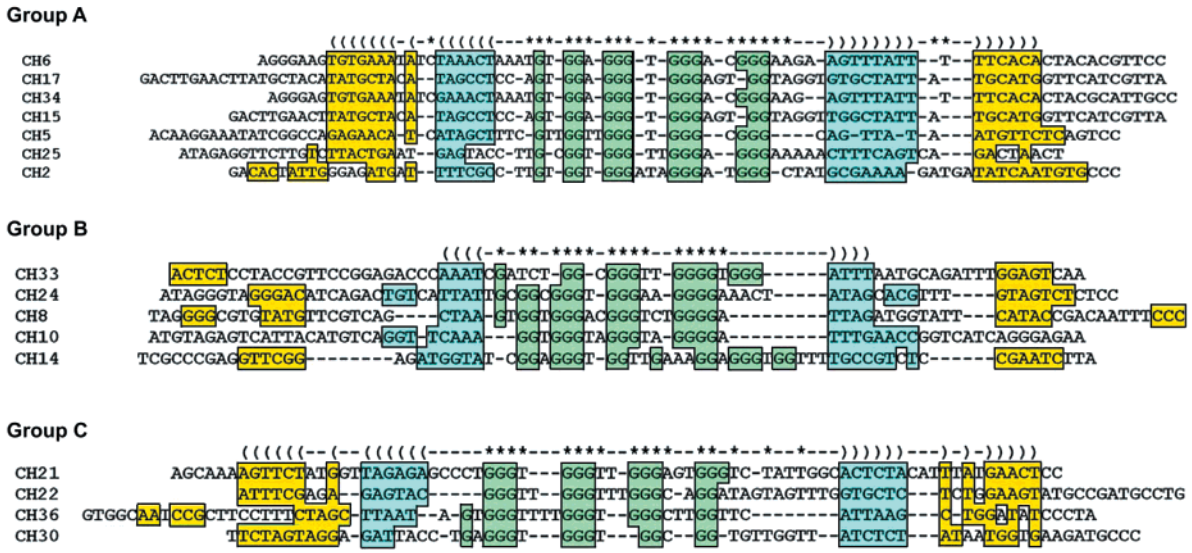

FIGURE 1: Sequence alignment of selected clones using the FOLDALIGN algorithm. Sequences are shown 5′ to 3′ and are grouped according to their highly conserved guanines shown in green. Flanking sequences predicted to form double-stranded regions are highlighted in yellow and in blue to their respective complementary regions, also indicated with parentheses above the sequence. (*) denotes high sequence conservation.

to reduce the possibility of nonspecific electrostatic interactions between cytochrome *c* and DNA that could occur at low ionic strengths. Whereas, as expected, the hemin-binding properties of the PS pool were excellent from the start of selection, cytochrome *c* binding increased substantially after the second round, and essentially reached a plateau following the fifth round. Starting from round 5, an additional step of negative selection was incorporated, in which DNA folded in the absence of hemin was applied to the cytochrome *c* column, and only those DNA molecules not binding to the column in the absence of hemin were allowed to continue through the selection. Following round 6, the DNA pool was cloned. Thirty-seven clones were sequenced and their random region sequences compared in search for sequence homologies that might be important for the binding of both hemin and cytochrome *c* (Figure 1). Since the starting library for this selection was the PS pool, described earlier, from a previous selection for porphyrin binding carried out by Li et al. (*12*), it was not surprising that guanine-rich sequence elements (shown in green boxes in Figure 1), consistent with porphyrin-binding sites, were found in all clones. However, unlike clones analyzed in the earlier selection (*12*), where the G-rich region within each clone was situated randomly within the N_{76} region, the G-rich regions within these clones appeared to be located centrally within the N_{76} sequence. These new clones also provided a stronger consensus sequence for the G-rich elements and could be classified into three groups based on their guanine consensus sequence. Members from Group A contained $GTG_2A(T)G_3TG_3AG_{2-3}$. Group B sequences ($GNG_2NG_3NG_3NG_4$) contained one run of four guanines, with two members containing an additional set of guanine triplets. Group C had in common $G_3T_nG_3T_nG_3NG_2$. Previous studies in our lab on DNA aptamer−porphyrin interactions (*12*, *15*) had found that these G-rich elements folded intramolecularly to form guanine quadruplexes (G-quadruplexes) (*29*, *30*). With the exception of the G-rich motif, however, attempts to find other elements of sequence homology among the new clones using conventional sequence alignment algorithms (*31*) failed.

However, despite the absence of overt sequence homology between the clones, when their sequences were subjected to a DNA folding prediction program (Mfold server, *32*), roughly half of the clones were predicted to fold in a similar way, forming one or two predominantly double-helical stems (involving sequences shown as boxed in Figure 1), with the guanine-rich, putatively hemin-binding element isolated as a terminal loop. With the aid of the sequence alignment tool FOLDALIGN (*21*, *22*), which takes into account secondary structure, we were able to identify conserved regions of base complementarity. Shown in Figure 1 in blue and yellow highlight, all sequences contained two sets of base-paired stems. Sequence homology of these stems is highest among Group A members, with runs of six to eight consecutive complementary bases. Sequences in Groups B and C had shorter conserved areas. Although the presence of two duplex stems is ubiquitous in the sequenced pool, the role of these elements in protein binding is unclear. Figure 2 shows the predicted secondary structure for a single representative clone, CH6, which was chosen for further characterization.

Spectroscopy of Hemin Binding. To investigate the importance for cytochrome or hemin binding of the putative stem regions flanking the G-rich element, two deletion mutants of clone CH6 were synthesized, which contained: (a) the full sequence of clone CH6, except for the 5′ and 3′ constant regions ("CH6A"), and (b) the full sequence minus the elements required for stem b as well as the 5′ and 3′ constant regions ("CH6B"). These are shown in Figure 2.

The binding of CH6 to hemin was measured by UV−visible spectroscopy, following the method of Travascio et al. (*15*). Figure 3A shows that disaggregated hemin binding to CH6 (or to CH6A or to CH6B, data not shown) gave rise to a hyperchromicity in the hemin Soret absorbance, along with a small red shift, from 398 to 404 nm. In addition, isosbestic points were seen at 420, 493, and 545 nm. The change in A_{404} as a function of DNA concentration was used to calculate dissociation constants, using the formalism of Wang et al. (*23*). Table 2 summarizes the K_d values for hemin binding to the three DNA oligomers. The values obtained

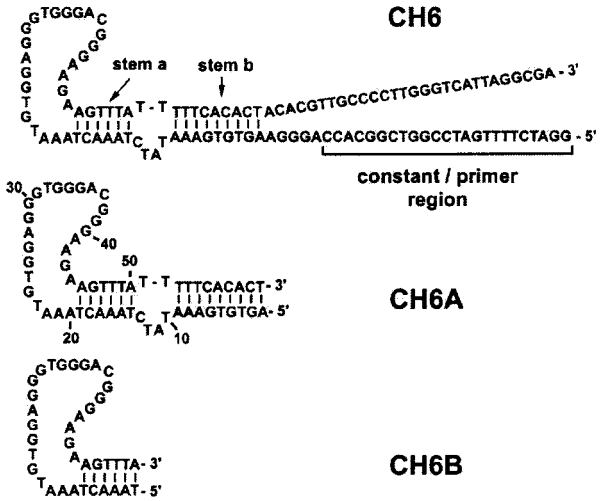

FIGURE 2: Sequence and the predicted folding of the DNA aptamer, CH6, and its two deletion mutants, CH6A and CH6B. Two double-helical stems separated by a four base bulge are predicted for CH6, based on sequence complementarity. CH6A lacks the primer-binding sequences of CH6, but maintains the two stems, a and b. CH6B lacks stem b, as well as the primer-binding sequences.

for CH6, CH6A, and CH6B were 3.56 ± 0.14, 0.97 ± 0.16, and 0.6 ± 0.22 μM, respectively. The extinction coefficients at 404 nm determined for the DNA−hemin complexes were 1.94×10^5, 1.98×10^5, and 1.56×10^5 M^{-1} cm^{-1}, respectively.

Scatchard analysis of hemin binding to CH6, CH6A, and CH6B gave ν values of 0.92, 0.86, and 1.12 ± 0.20, respectively (where ν describes the number of moles of hemin bound per mole of DNA). This indicated that for all three DNA oligomers, one hemin molecule bound per molecule of DNA.

Binding of Cytochrome c to CH6A Monitored by Difference Spectroscopy. The docking of protein partners to cytochrome *c* has traditionally, and most conveniently, been measured using "difference" spectroscopy (*24*−*26*), the measurement of small spectroscopic perturbations in the spectra of the cytochrome's heme concomitant with the docking of another protein to cytochrome *c*. Fundamentally, this involves obtaining the difference between the spectrum of the cytochrome *c*−docking partner complex and the added individual spectra of cytochrome *c* and of its docking partner.

We used difference spectroscopy in the Soret region of the spectrum to measure the binding affinity of cytochrome *c* to CH6 and to its deletion mutants. The binding of cytochrome *c* to 1 μM CH6A (in both the presence and absence of hemin) resulted in positive difference absorbance spectra. Figure 4A shows the spectrum obtained in the presence of hemin (dashed line). A major peak was seen at 407 nm (as well as two smaller maxima at approximately 500 and 530 nm in the presence of hemin). In the absence of hemin (solid line), the difference spectrum was similar, with the exception of a lower absorbance of the Soret peak (409 nm) relative to that seen in the presence of hemin. The maximal change in the spectra amounted to ~2% of the total absorbance (with $\Delta\epsilon_{408} = 1.02 \times 10^4$ M^{-1} cm^{-1}). Figure 4B plots ΔA_{408} against the molar ratio of cytochrome *c* to CH6A DNA in the presence (filled circles) and absence (open circles) of hemin. Saturation of the absorbance difference occurred at a protein to DNA molar ratio of ~1, suggesting

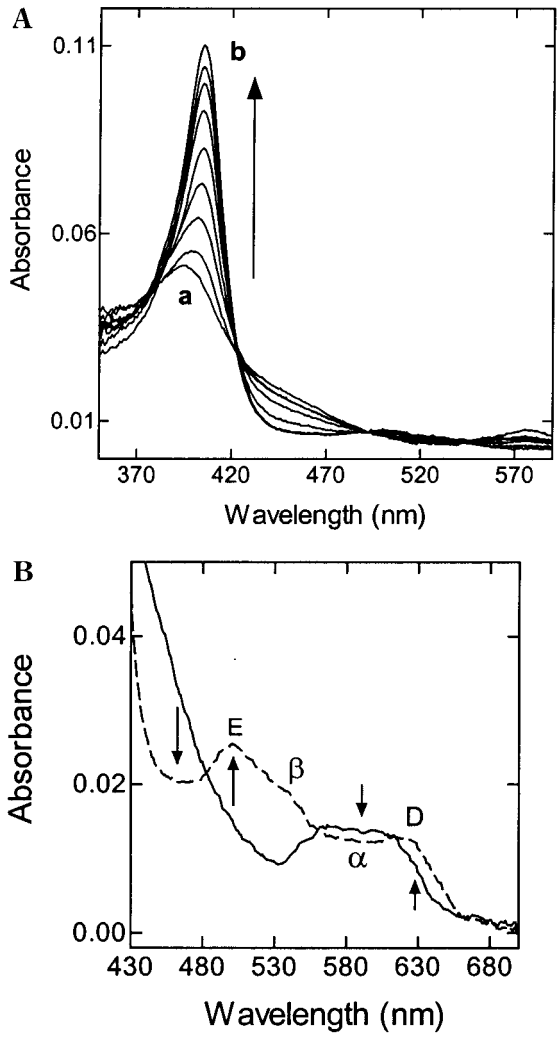

FIGURE 3: (A) Binding of hemin to the aptamer CH6. The absorbance spectrum of hemin is plotted as a function of increasing DNA concentrations. The hemin concentration was held constant at 0.5 μM, and the DNA concentration varied from 0 to 1, 2, 5, 10, 15, and 20 μM (a = 0 μM; b = 20 μM DNA). (B) Spectra of the visible region of DNA-complexed hemin and free hemin. 1.5 μM hemin (solid lines) in buffer A (see Materials and Methods) and 20 μM CH6A DNA folded with 1.5 μM hemin in buffer A (dashed line).

Table 2: Summary of Dissociation Constants (K_D)[a]

	CH6	CH6A	CH6B
DNA to hemin[b]	3.6 ± 0.2	1.0 ± 0.2	0.6 ± 0.2
DNA to cyt c[c]	0.8 ± 0.3	4.6 ± 0.6	ND
DNA to cyt c in presence of hemin[d]	0.4 ± 0.2	0.3 ± 0.2	ND

[a] K_D values are stated in μM. [b] Buffers conditions used: 10 μM hemin, 50 mM Tris-HCl, pH 8.0, 120 mM NaCl, 20 mM KCl, 1% DMSO, and 0.03% Triton X-100. [c] Conditions same as in footnote *b* without hemin and with 10 μM ferricyanide. [d] Conditions same as in footnote *c*, with the addition of 10 μM hemin.

a binding stoichiometry of one cytochrome *c* molecule to one molecule of CH6A (similarly, analysis of cytochrome binding to the larger CH6 also gave a 1:1 protein:DNA binding stoichiometry; data not shown). The stoichiometries found agreed with Scatchard analysis and Job plots (*33*) (data not shown). Figure 4B shows also that CH6A bound cytochrome *c* with a significantly higher affinity in the presence

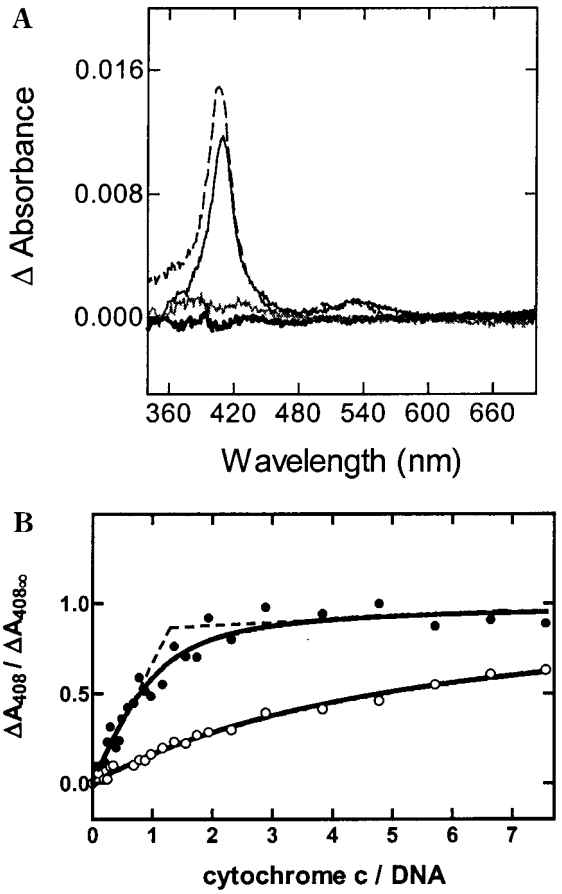

FIGURE 4: (A) Electronic difference spectra of 1 μM CH6A in the presence of cytochrome *c*. A major Soret peak is observed for CH6A folded with 10 μM hemin (dashed line) and for CH6A alone (solid line), but none for CH6B (thick line) or PS2M (gray line), both in the presence of 10 μM hemin. (B) Absorbance difference at 408 nm of CH6A hemin titrated with increasing concentrations of cytochrome *c*. The absorbance difference saturates at a DNA: cytochrome molar ratio of 1.1. Titrations were carried out on 1 μM CH6A DNA, in the presence (●) and absence (○) of 10 μM hemin, in selection buffer A.

of hemin ($K_d = 0.3$ μM) than in the absence of hemin ($K_d =$ 4.6 μM).

While difference spectra were observed with CH6A and CH6, the oligomer CH6B failed to produce a difference spectrum (Figure 4A, thick line), suggesting a lack of significant binding of cytochrome *c* to CH6B. This striking difference in the properties between CH6A and CH6B may indicate (1) that either stem b of the aptamer secondary structure (see Figure 2) is directly involved in binding to cytochrome *c* or (2) that stem b helps stabilize the overall folded structure of the molecule, possibly stabilizing stem a such as to facilitate binding to the protein. As a control, we also attempted to determine if PS2M (*15*−*18*), a hemin-binding 18-mer that folds to form a quadruplex with no double-stranded elements, was capable of producing a difference spectrum. Both in the presence of hemin (Figure 4A, gray line) and in the absence of hemin (data not shown), PS2M did not produce a difference spectrum in the presence of cytochrome *c*. Table 2 summarizes the dissociation constants for complexes formed by the aptamer oligomers to hemin alone, to cytochrome *c* alone, and to hemin and cytochrome *c* in a ternary complex. Because of the 1:1 hemin:CH6A binding stoichiometry, as well as the interesting feature of enhanced binding affinity in the presence of hemin, the aptamer oligomer CH6A was chosen for a more in-depth analysis.

DNA Structure Probing. Chemical probing analysis was carried out with dimethyl sulfate (DMS) and diethyl pyrocarbonate (DEPC) on CH6A and on complexes of CH6A with hemin and/or cytochrome *c*. DMS preferentially methylates the N7 position of guanines, accessible from the major groove within Watson−Crick double helices. Therefore, the interaction of proteins with the major groove of DNA duplexes can be footprinted using DMS. However, DMS reactivity also provides information about the participation of specific guanines in guanine quartet formation (guanines in G-quartets are not methylated by DMS) (*34*). DEPC reacts with adenine N7 positions, but preferentially with adenines that are present in either single-stranded, unstructured, or solvent-exposed regions of DNA secondary/tertiary structure. Figure 5A shows the DMS modification pattern of CH6A under different conditions. In the low-salt TE buffer (lane 1), all guanines in CH6A showed DMS reactivity. Folding of CH6A in a K^+-containing buffer (lane 2) still left all guanines reactive, even though it is known that the potassium ion supports the formation as well as stabilization of guanine quartets. However, when hemin was added (lane 3) to CH6A in the potassium buffer, significant protection was seen for the central region of guanines, from G24 to G40, consistent with the anticipated hemin-binding, guanine-rich loop (Figure 2) folding to form a G-quadruplex. The addition of cytochrome *c* to the CH6A−hemin complex (lane 4) did not significantly alter the guanine modification pattern. However, the addition of cytochrome *c* in the absence of hemin (lane 5) still showed significant guanine reactivity with DMS, suggesting that cytochrome *c* binding did not in itself support G-quadruplex formation. In correlation with this finding were the binding data to CH6A (above), which indicated that the prior, and hemin-assisted, formation of a G-quadruplex resulted in a stronger binding of cytochrome to CH6A. Lane 6 shows that adding cytochrome *c* first, followed by hemin, to CH6A gave a protection pattern essentially indistinguishable from that seen in lane 4 (where hemin was added first, followed by cytochrome). Therefore, the order of addition of the two ligands, hemin and cytochrome *c*, to CH6A was probably not important for the proper formation of the ternary complex.

The DEPC experiments (Figure 5B) show that A15−A17 became protected when folded in K^+ buffer (lane 8 versus lane 7), consistent with their lying within a duplex region (see Figure 2). When hemin was added to this solution (lane 9, Figure 5B), A28 and A36 within the G-rich region became hyper-reactive, possibly owing to being thrust out into the solvent concomitant with their surrounding guanines base-pairing with each other to form the quadruplex. The addition of cytochrome *c* to this DNA−hemin complex (lane 10) again gave a reactivity/protection pattern essentially unchanged from that in lane 9. Cytochrome, added in the absence of hemin (lane 11), did not result in the hyperactive adenines seen in lanes 9 and 10, once again suggesting that cytochrome *c* in itself was incapable of supporting the formation of the G-quadruplex. As seen with the DMS experiments, reversing the order of hemin and cytochrome *c* addition (lane 12) did not result in a different protection pattern from the one seen in lane 10.

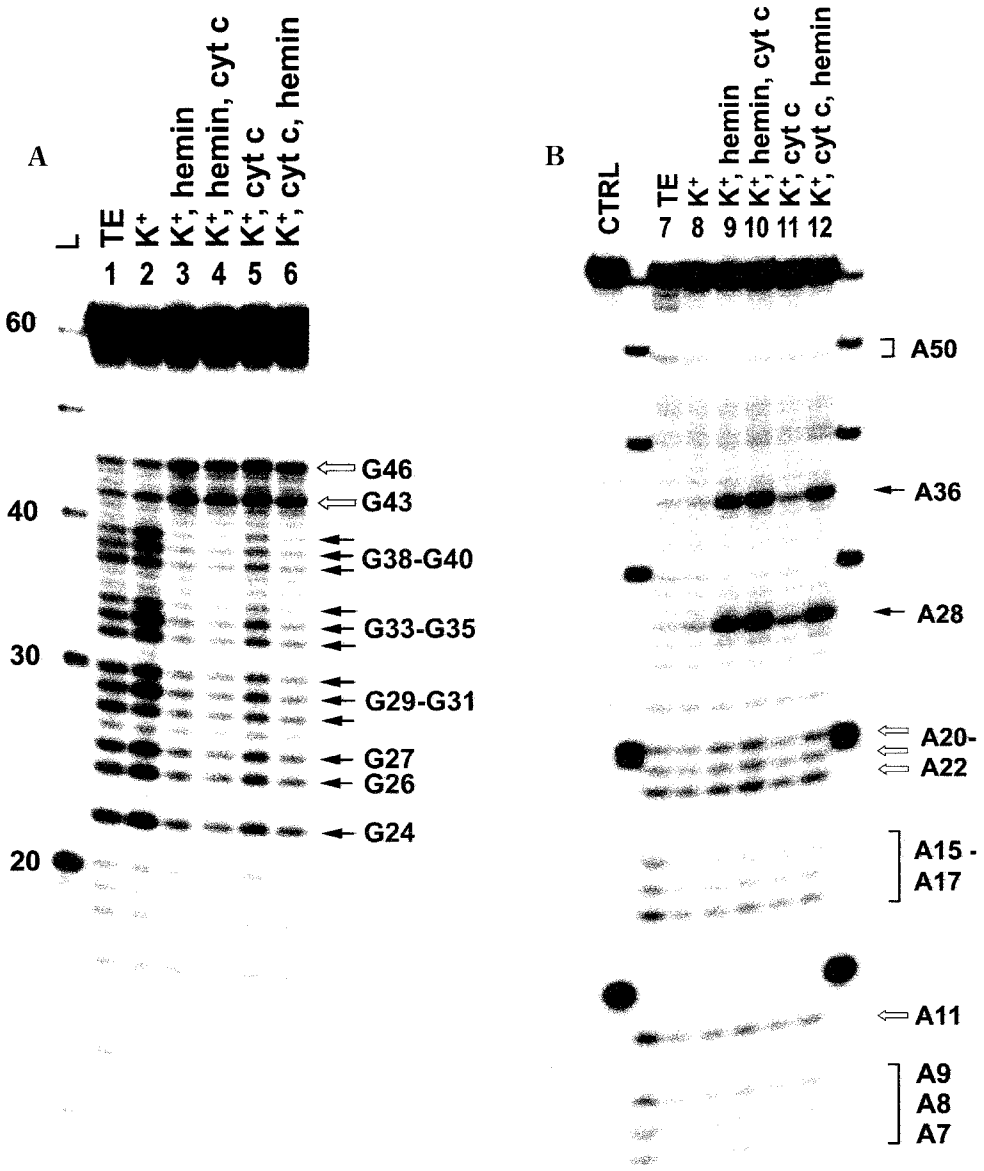

FIGURE 5: Chemical probing analysis of (A) DMS-modified and (B) DEPC-modified CH6A, following treatment with piperidine. Samples in lanes 1 and 7 were probed in TE buffer. Lanes 2 and 8: DNA folded in methylation buffer (containing 20 mM K^+). Lanes 3 and 9: 5 μM hemin added to DNA folded in methylation buffer. Lanes 4 and 10: 10 μM cytochrome *c* added to DNA−hemin in methylation buffer. Lanes 5 and 11: 10 μM cytochrome *c* added to DNA folded in methylation buffer in the absence of hemin. Lanes 6 and 12: 5 μM hemin added to DNA folded in buffer with 10 μM cytochrome *c*. Lane C is a DEPC control where nonmodified DNA is subject to piperidine treatment. Solid arrows indicate areas of protection in (A) and areas of hyper-reactivity in (B). Open arrows indicate bases showing little or no change. Bracketed regions show regions following the addition of methylation buffer alone. Little change is seen when buffer alone is added to the DNA (lanes 1, 7 versus 2, 8). Protection of central guanines is seen when hemin is added (lane 3) and correlates with the appearance of hyper-reactive adenines 28 and 36 (lane 9).

Fenton Reaction Footprinting. The chemical probing experiments utilizing DMS and DEPC (above), which monitor the conformation of individual bases in the DNA and also the hydrogen-bonding or other contacts made by the DNA bases, did not yield any obvious signature for the binding of cytochrome *c* to CH6A (Figure 5). We therefore attempted to 'footprint' this interaction using hydroxyl radicals generated in situ by the Fenton reaction (*28*). Hydrogen abstraction from the 1′-position of the deoxyribose sugars of DNA leads to a breakage of the DNA chain; and hydroxyl radicals are therefore useful as probes for the sugar−phosphate backbone of DNA, rather than for the bases. Figure 6 shows that the pattern of cleavage changed relatively slightly when the CH6A DNA was folded in potassium buffer, either in the absence (lane 2) or in the presence (lane 3) of hemin. When cytochrome *c* was added to the DNA−hemin complex (lane 4), however, a clear footprint was observed from residues ~40 to 55. This protected stretch lies just outside of the G-quadruplex-forming region, but incorporates a portion of the double-helical region (as predicted, shown in Figure 2, and also from the DEPC-protection experiments, Figure 5B). Once again, the order of addition of hemin and cytochrome *c* appeared not to be important (lanes 4 and 6)—both orders of addition generated the footprint. However, cytochrome *c* in the absence of hemin (lane 5) did not generate the unequivocal footprint seen in the dual presence of hemin and cytochrome. As an added control to test for the specific locus of cytochrome binding upon the DNA, we used a highly basic peptide known to bind to RNA (*35*). ADP-1 is a 36 amino

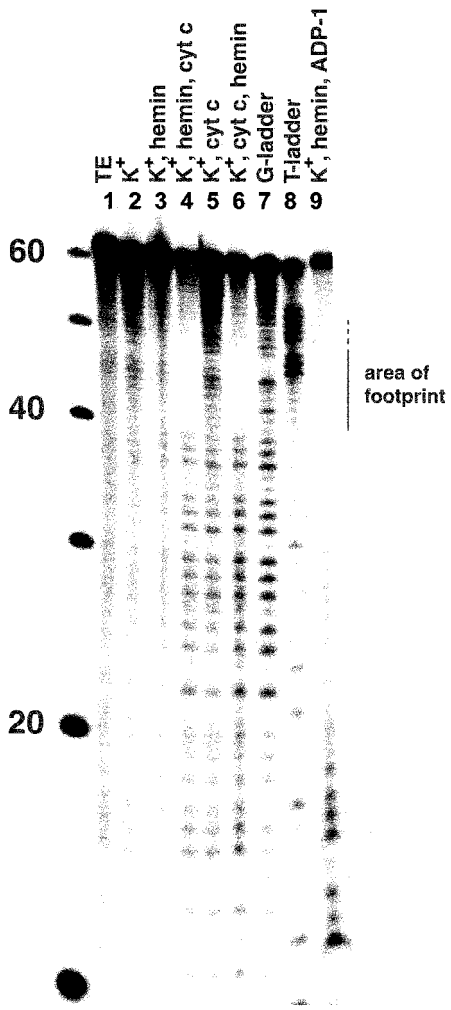

FIGURE 6: Fenton reaction footprinting analysis of CH6A. 0.5 μM CH6A was folded in selection buffer A (containing 140 mM monovalent salt). The reaction was initiated by the addition of 10 μM H_2O_2 and quenched with 5 mM thiourea. Samples were run in a 10% denaturing gel. 'G' and 'T' lanes (lanes 7 and 8) show the G and T sequencing ladders, respectively. Lane 1: DNA in TE buffer. Lane 2: DNA folded in selection buffer A (containing 20 mM K^+). Lane 3: 10 μM hemin added to folded DNA. Lane 4: 10 μM cytochrome *c* added to DNA folded with hemin. Lane 5: 10 μM cytochrome *c* added to DNA folded in the absence of hemin. Lane 6: the order of hemin and cyt *c* addition was reversed. In the dual presence of hemin and cyt *c* (lanes 4 and 6), a footprint could be seen, indicated by the bracketed region. Lane 9: control reaction with 12 μM ADP-1 peptide added to hemin-folded CH6A.

acid arginine-rich peptide that corresponds to the 37−72 amino acid region of the HIV Tat protein. ADP-1 might be expected to bind promiscuously, via mainly Coulombic interactions, with the aptamer DNA. Lane 9 shows the footprint produced when incubating hemin-complexed CH6A with 12 μM ADP-1. The very large footprint produced by the small peptide is indicative of a high degree of binding, yet largely non-site-specific interaction. The stoichiometry of binding is most likely estimated to be much larger than 1:1.

DISCUSSION

Binding of Hemin to the DNA Aptamer. Earlier searches for single-stranded DNA (and RNA) sequences capable of folding to form porphyrin-binding sites (*12*, *15*) had found guanine-rich sequences, that folded to form G-quadruplexes, to be important for such binding sites. The precise mode of interaction of hemin with such quadruplex sites has not been elucidated, but it has been proposed, from energetic considerations, that the preferred binding site of a porphyrin (or metalloporphyrin) to a quadruplex may be via stacking interactions upon the terminal guanine quartets of a quadruplex, rather than via intercalation between quartets (*15*−*17*). The observed hyperchromicity and sharpening of the porphyrin Soret absorption upon binding to a quadruplex has previously been attributed to the porphyrin being in a more hydrophobic environment (*14*, *15*). The methylation and carboxyethylation probing (using DMS and DEPC) data obtained with the CH6A aptamer are fully consistent with the conserved guanine-rich region (a) being the hemin-binding site and (b) forming a guanine-quadruplex folded structure. Although the precise mode of interaction of hemin with CH6A DNA was not yet clear, a key feature of *this* aptamer (as compared to those analyzed in previous work; *12*, *15*−*17*) was that the formation of its folded quadruplex structure required the binding of hemin. In other words, hemin binding to CH6 or its deletion mutants appeared to operate via an induced fit mechanism, where ligand binding itself contributed to the formation of the binding site.

Analysis of the visible region of the DNA−hemin complex spectrum, shown in Figure 3B, indicated a marked similarity with that of the previously characterized PS2M DNA−hemin complex (*15*−*17*). Absorption peaks were observed at 630 and 500 nm, corresponding to the D and E bands, respectively, along with a general decrease in the α band region. Travascio and Sen (*14*) had previously attributed these changes to the presence of ligand-to-metal charge-transfer transitions, with the heme being a hexacoordinate high-spin species. Extensive EPR work had demonstrated that axial ligation of the iron center was mediated by a water molecule and, probably, a guanine residue within the oligonucleotide (*17*, *18*). Given the similarity of the spectra of the previously characterized PS2M−heme complexes to the DNA−heme complex reported here, as well as the guanine-rich nature of both PS2.M and CH6A, it is expected that the heme in the CH6A−hemin complex also exists as a high-spin hexacoordinate species. Further experiments will help to confirm this.

Binding of Cytochrome c to the DNA Aptamer. The binding of cytochrome *c* to its normal biological redox partners has been studied using difference spectroscopy methods, under ionic conditions similar to the ones used in this study. The binding of cytochrome *c* to cytochrome *c* peroxidase was determined to have a K_d of 2 mM at an ionic strength of 200 mM (*24*). K_d values for the binding of cytochrome *c* to cytochrome *c* oxidase ranged from 0.3 to 3.0 μM at an ionic strength of 100 mM and from 8 nM to 1 μM at a 50 mM ionic strength (*26*). The association of these proteins is highly sensitive to the ionic strength of the solution, with optimal binding (as might be expected for proteins interacting mainly electrostatically) at very low salt concentrations. The dissociation constants that we have measured for the binding of cytochrome *c* to our DNA−hemin complex are within the range of these values.

The DMS and DEPC protection studies, which did not yield a clear footprint of the binding of cytochrome *c*, suggested that interaction of the protein with the DNA was not primarily through contacts to the 'major groove face' of

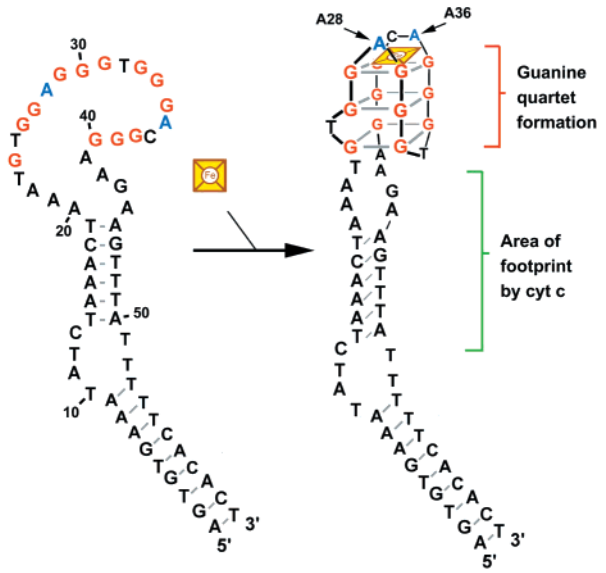

FIGURE 7: Proposed structural model for the binding of cytochrome and hemin to CH6A DNA.

individual adenine or guanine bases. Footprinting using hydroxyl radicals, however, indicated that the binding of cytochrome *c* rendered the sugar−phosphate backbone of a stretch of 12−15 nucleotides on CH6A significantly less accessible to solvent. According to the folding scheme shown in Figure 2, and the DEPC protection results (Figure 5B), elements of this sequence stretch should fold to form a duplex. However, the hydroxyl footprinting evidence did suggest that the cytochrome *c* interaction was mainly with one of the two strands (nucleotides ~40 to ~55 of CH6A, but not so well with nucleotides ~10 to ~25; see Figures 6 and 7) of the putative part-duplex flanking the hemin-binding quadruplex.

To conceptualize how a single molecule of cytochrome *c* (with a diameter of ~40 Å at its longest axis) might produce such a 15 nucleotide footprint, the DNA could be partially wrapped around the protein, with the single-stranded regions affording flexibility to kink the duplex elements. Figure 8 shows a model for this proposed interaction. Horse heart cytochrome *c* is known to contain 19 lysine and 2 arginine residues, whose positively charged side chains could interact electrostatically with the negatively charged phosphates of the DNA backbone. Such a purely electrostatic interaction, however, would be expected to be somewhat nonspecific. In studies of sequence-specific DNA-binding proteins, it has been found that direct and water-mediated hydrogen bonds between the protein side chains and the DNA bases and backbone are important for specific recognition (*36*, *37*). Studies on RNA interactions with proteins (*38*−*41*) have indicated that along with significant conformational changes that occur within the RNA itself, there are also base−amino acid side chain contacts that afford specificity. It is also possible that in the CH6A−cytochrome interaction a degree of specificity may be afforded by direct (possibly hydrogen-bonding) interactions between the cytochrome side chains and the DNA phosphate groups as well as functionalities on the DNA bases that are not subject to the DMS and DEPC footprinting assays.

The role of the G-quadruplex domain in positioning the cytochrome *c* on CH6A is hard to gauge at this point,

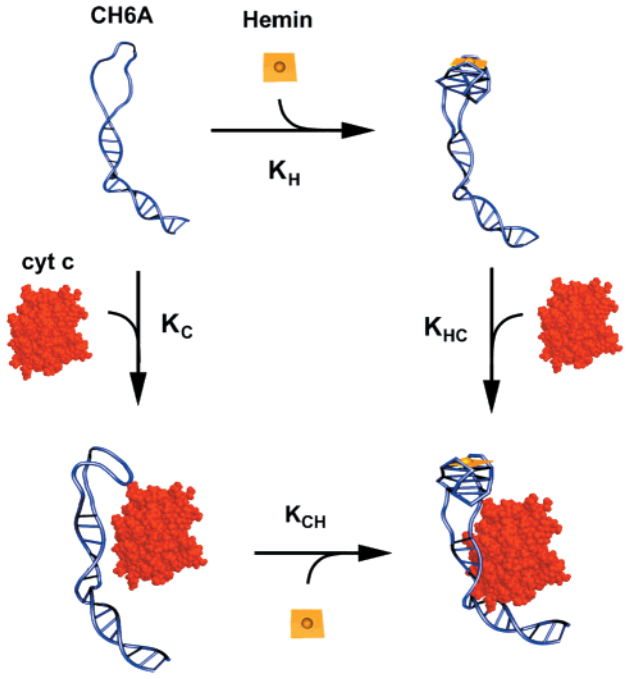

FIGURE 8: Thermodynamic pathways toward the formation of the ternary complex, CH6A−hemin−cytochrome *c*. Cytochrome *c* structure taken from NMR structure coordinates (*57*) in the Brookhaven Protein DataBank and exported from RasMol viewer.

although it is important to emphasize that G-quadruplexes have twice the negative charge density per unit length compared to double helices (*29*, *30*); therefore, in terms of having a higher electrostatic potential per unit length (relative to a duplex), a G-quadruplex would be an excellent site for interaction by the positively charged cytochrome *c*. There are also a number of proteins that have been reported to bind G-quadruplex structures (*42*−*46*), including thrombin (*42*), HIV1 integrase (*46*), and fd gene 5 protein (*45*). However, in our studies, the hydroxyl radical footprint of cytochrome *c* binding (Figure 6) does not indicate extensive backbone sugar−phosphate protection for the quadruplex nucleotides; moreover, interactions of the protein with the grooves of the quadruplex are not amenable to footprinting by DMS or DEPC, since the DMS- and DEPC-reactive guanine N7 functionalities are already resistant to modification owing to their participation in quartet formation.

Allostery in the Binding of the Two Ligands. Recently, a number of papers have reported allosteric behavior in nucleic acids. Most of these involve the binding of a single ligand to a nucleic acid molecule, with a concomitant change in the structure and/or properties of the nucleic acid distal from the ligand-binding site. The allosteric variants of the hammerhead ribozyme developed by Breaker and colleagues are the best examples of this (reviewed in *47*). Other examples include the selection of an allosteric RNA-cleaving ribozyme responsive to doxycycline (*48*), and the selection of an allosteric RNA ligase responsive to an ATP cofactor (*49*).

Recently, however, Jose et al. (*50*) have reported the construction of a variant of the hammerhead ribozyme that requires the binding of two effectors, flavin mononucleotide (FMN) and theophylline, for catalysis of phosphodiester bond cleavage. In their modular design, the hammerhead motif as a catalytic entity was conjoined to two different and proximal binding sites for the two effectors. The hammerhead motif

has also been used in developing dimeric ribozymes, termed 'maxizymes', that can respond to RNA effector molecules both in vitro and in vivo (*51*). In a different approach, two separate RNA selection pools for binding to Cibacron blue and cholic acid, respectively, were fused together (*52*). The resultant pool was then reselected for allosteric behavior, such that the binding of one ligand negatively affected the binding of the other.

In our system, as shown above, the binding of hemin to the DNA aptamer stimulates the binding of cytochrome *c* to the aptamer. Figure 8 shows a thermodynamic cycle for the binding of the two ligands to the aptamer, i.e., the two possible pathways to the ternary complex, CH6A−hemin−cytochrome *c*. The two pathways describe a different order of binding of the two ligands. In this paper, we report values for three of the four equilibrium (association) constants, K_H, K_C, and K_{HC}, shown in Figure 8. We were unable to find a convenient or reliable method for measuring the fourth equilibrium constant, K_{CH}. In this paper, we report that $K_{HC} > K_C$ (i.e., the hemin−DNA complex binds cytochrome *c* more strongly than does the DNA itself). The thermodynamic cycle therefore mandates that $K_{CH} > K_H$ (in other words, the cytochrome *c*−DNA complex should bind hemin more strongly than the uncomplexed DNA binds hemin). In future experiments, we will attempt to measure directly the equilibrium constant K_{CH}.

Spatial Relationship between Hemin and Cytochrome c within the Ternary Complex. The binding of CH6A DNA (in the absence *or* presence of complexed hemin) to cytochrome *c* was observed to perturb the electronic absorption spectrum of cytochrome *c*. This phenomenon has been observed in other studies, of cytochrome *c* binding to its protein redox partners cytochrome b_5 (*25*), cytochrome *c* oxidase (*26*), and cytochrome *c* peroxidase (*24*), as well as to monoclonal antibodies specific for cytochrome *c* (*53*). Positive difference spectra in the Soret peak are believed to be the results of a change in the local environment of the exposed heme crevice of cytochrome *c* (*53*). The data presented in this paper suggest that a DNA−hemin complex is able to perturb the cytochrome *c* spectrum in a way comparable to the perturbation caused by the docking to cytochrome *c* of its various hemoprotein electron-transfer partners. This raises the possibility of electron transfer between the two heme centers in this ternary complex, separated presumably by both protein and DNA, and raises questions of what the most optimal path might be for such a transfer. Future experiments will be sought on the ternary complex, including spectroscopic studies and determining the distance between the two iron centers.

Implications for an RNA World. A theoretical gap exists between the proposed first signs of life of a putative "RNA World" (*54*) and the first cellular life possibly resembling modern archaebacteria. Many of these bacteria were able to survive in the extreme and anaerobic conditions of the early Earth environment, metabolize sulfur and nitrogen as a food source, and survive in extreme heat, high salt, or high pH. Extant archaebacteria that live under these conditions have evolved proteins that bind metalloporphyrins as well as other redox cofactors to carry out their reduction/oxidation reactions (*55*, *56*). In a possible transition from the RNA world to a protein-nucleic acid world, some period may have existed where nucleic acids, with the help of cofactors, may have participated in the redox processes that would eventually be superseded by proteins. Currently there is little known about direct molecular interactions between nucleic acids and electron-transfer proteins, although a number of these proteins do use nucleotide-like cofactors. The ability of a DNA molecule to bind hemin and then recognize an electron-transfer protein offers a prototype for investigating the ability of nucleic acids to participate in electron-transfer reactions.

ACKNOWLEDGMENT

We are grateful to Dr. Yingfu Li, Dr. Paola Travascio, and the members of the Sen laboratory. We also thank Dr. Grant Mauk (Department of Biochemistry and Molecular Biology, University of British Columbia) for discussions on cytochrome *c*, as well as Dr. Dominic Zichi (Somalogic, Boulder, CO) for his advice on sequence analysis algorithms.

REFERENCES

1. Pettigrew, G. W., and Moore, G. R. (1987) *Cytochromes c: Biological Aspects*, Springer-Verlag, New York.
2. Cai, J., Yang, J., and Jones, D. P. (1998) *Biochim. Biophys. Acta 1366*, 139−149.
3. Mignotte, B., and Vayssiere, J. L. (1998) *Eur. J. Biochem. 252*, 1−15.
4. Green, D. R., and Reed, J. C. (1998) *Science 281*, 1309−1312.
5. Mauk, A. G., Mauk, M. R., Moore, G. R., and Northrup, S. H. (1995) *J. Bioenerg. Biomembr. 27*, 311−330.
6. Stemp, E. D. A., and Barton, J. K. (2000) *Inorg. Chem. 39*, 3868−3874.
7. Li, Y., and Breaker, R. R. (1999) *Curr. Opin. Struct. Biol. 9*, 315−323.
8. Sen, D., and Geyer, C. R. (1998) *Curr. Opin. Chem. Biol. 2*, 680−687.
9. Breaker, R. R., and Joyce, G. F. (1994) *Curr. Biol. 1*, 223−229.
10. Li, Y., Liu, Y., and Breaker, R. R. (2000) *Biochemistry 39*, 3106−3114.
11. Unrau, P. J., and Bartel, D. P. (1998) *Nature 395*, 260−263.
12. Li, Y., Geyer, C. R., and Sen, D. (1996) *Biochemistry 35*, 6911−6922.
13. Li, Y., and Sen, D. (1996) *Nat. Struct. Biol. 3*, 743−747.
14. Li, Y., and Sen, D. (1998) *Chem. Biol. 5*, 1−12.
15. Travascio, P., Li, Y., and Sen, D (1998) *Chem. Biol. 5*, 505−517.
16. Travascio, P., Bennet, A., Wang, D., and Sen, D. (1999) *Chem. Biol. 6*, 779−787.
17. Travascio, P., Witting, P., Mauk, G., and Sen, D. (2001) *J. Am. Chem. Soc. 123*, 1337−1348.
18. Witting, P. K., Travascio, P., Sen, D., and Mauk, A. G. (2001) *Inorg. Chem. 40*, 5017−7023.
19. Stonehuerner, J., Williams, J. B., and Millett, F. (1979) *Biochemistry 18*, 5422−5427.
20. Brautigan, D. L., Ferguson-Miller, S., and Margoliash, E. (1978) *Methods Enzymol. 53*, 128−164.
21. Gorodkin, J., Heyer, L. J., and Stormo, G. D. (1997) *Nucleic Acids Res. 25*, 3724−3732.
22. Gorodkin, J., Heyer, L. J., and Stormo, G. D. (1997) in *Proceedings of the Fifth International Conference on Intelligent Systems in Molecular Biology* (Gaasterland, T., Kerp, P., Karplus, K., Ouzounis, C., Sander, C., and Valencia, A., Eds.) pp 120−123, AAAI Press, Menlo Park, CA.
23. Wang, Y., Hamasaki, K., and Rando, R. R. (1997) *Biochemistry 36*, 768−779.
24. Erman, J. E., and Vitello, L. B. (1980) *J. Biol. Chem. 255*, 6224−6227.
25. Mauk, M. R., Reid, L. S., and Mauk, A. G. (1982) *Biochemistry 21*, 1843−1846.
26. Michel, B., and Bosshard, H. R. (1984) *J. Biol. Chem. 259*, 10085−10091.
27. Falk, J. E. (1975) *Porphyrins and Metalloporphyrins* (Smith, K. M., Ed.) Elsevier Publishing Co., Amsterdam.

28. Weidner, M. F., Millard, J. T., and Hopkins, P. B. (1989) *J. Am. Chem. Soc. 111*, 9270−9272.
29. Wellinger, R., and Sen, D. (1997) *Eur. J. Cancer 33*, 735−749.
30. Willamson, J. R. (1994) *Annu. Rev. Biophys. Biomol. Struct. 23*, 703−730.
31. Higgins, D. G., Thompson, J. D., and Gibson, T. J. (1996) *Methods Enzymol. 266*, 383−402.34.
32. SantaLucia, J., Jr. (1998) *Proc. Natl. Acad. Sci. U.S.A. 95*, 1460−1465.
33. Job, P. (1928) *Ann. Chim. 9*, 113−203.
34. Sen, D., and Gilbert, W. (1988) *Nature 334*, 364−366.
35. Churcher, M. J., Lamont, C., Hamy, F., Dinwall, C., Green, S. M., Lowe, A. D., Butler, P. J., Gait, M. J., and Karn, J. (1993) *J. Mol. Biol. 230*, 90−110.
36. Seeman, N. C., Rosenberg, J. M., and Rich, A. (1976) *Proc. Natl. Acad. Sci. U.S.A. 73*, 804−805.
37. Pabo, C., and Sauer, R. (1992) *Annu. Rev. Biochem. 61*, 1053−1095.
38. Leulliot, N., and Varani, G. (2001) *Biochemistry 40*, 7947−7956.
39. Aboul-ela, F. A., Karn, J., and Varani, G. (1995) *J. Mol. Biol. 253*, 313−332.
40. Aboul-ela, F. A., Karn, J., and Varani, G. (1996) *Nucleic Acids Res. 24*, 3974−3981.
41. Puglisi, J. D., Tan, R., Canlan, B. J., Frankel, A. D., and Williamson, J. R. (1992) *Science 257*, 76−80.
42. Fang, G., and Cech, T. R. (1993) *Biochemistry 32*, 11646−11657.
43. Macaya, R. F., Schultze, P., Smith, F. W., Roe, J. A., and Feigon, J. (1993) *Proc. Natl. Acad. Sci. U.S.A. 90*, 3745−3749.
44. Arimondo, P. B., Riou, J. F., Mergny, J. L., Tazi, J., Sun, J. S., Garestier, T., and Helene, C. (2000) *Nucleic Acids Res. 28*, 4832−4838.
45. Oliver, A. W., Bogdarina, I., Schroeder, E., Taylor, I. A., and Kneale, G. G. (2000) *J. Mol. Biol. 301*, 575−584.
46. Jing, N., Marchand, C., Liu, J., Mitra, R., Hogan, M. E., and Pommier, Y. (2000) *J. Biol. Chem. 275*, 21460−21467.
47. Soukup, G. A., and Breaker, R. R. (2000) *Curr. Opin. Struct. Biol. 10*, 318−325.
48. Pagineau, N., Jenne, A., Thuillier, V., and Famulok, M. (2000) *Angew. Chem., Int. Ed. Engl. 39*, 23, 4369−4373.
49. Robertson, M. P., and Ellington, A. D. (1999) *Nat. Biotech. 17*, 62−66.
50. Jose, A. M., Soukup, G. A., and Breaker, R. R. (2001) *Nucleic Acids Res. 29*, 1631−1637.
51. Warashina, M., Kuwabara, T., and Tiara, K. (2000) *Structure 8*, R207−R212.
52. Wu, L., and Curran, J. F. (1999) *Nucleic Acids Res. 27*, 1512−1516.
53. Raman, C. S., Jemmerson, R., Nall, B. T., and Allen, M. J. (1992) *Biochemistry 31*, 10370−10379.
54. Gilbert, W. (1986) *Nature 319*, 618.
55. Thauer, R. K. (1998) *Microbiology 144*, 2377−2406.
56. Schäfer, G., Engelhard, M., and Müller, V. (1999) *Microbiol. Mol. Biol. Rev. 63*, 570−620.
57. Banci, L., Bertini, I., Gray, H. B., Luchinat, C., Reddig, T., Rosato, A., and Turano, P. (1997) *Biochemistry 36*, 9867−9877.

BI015785F